Elastic modeling and reverse time migration

Ziguang Su and Daniel Trad

ABSTRACT

In an elastic medium, reverse time migration (RTM) uses the velocity-stress method for the wavefield propagation and a numerical seismic source to create shot and receiver wavefields required in the imaging conditions. This essay discusses different ways to introduce a seismic source in the elastic modeling process. The seismic source in the elastic reverse time migration/RTM is normally expressed by a combination of wavelet functions in spatial and time dimensions. In most occasions, pure P/S wave sources are preferred. This paper shows that the typical way to introduce the source in RTM is not a pure P/S wave source. A better approach to approximate pure P/S modes is to use a plane source. In this paper, we use elastic modeling process to generate P&S shot records. Then we use acoustic RTM and least squares RTM to migrate these elastic data, using P and S velocities in different experiments. In both cases, the reflectivity models obtained from RTM are very poorly defined, but the LSRTM produces a clean image because of its capability to filter out events that can not be properly predicted by the modeling operator.

INTRODUCTION

Velocity-stress method

The velocity-stress method is a way to compute wavefield propagation in the elastic medium where stress tensor σ_{xx}, σ_{xz}, σ_{zz}, and velocities v_x, v_z are computed by the finite difference in a staggered grid (Virieux, 1986). The stress-strain relationship is

$$
\begin{aligned}
\sigma_{xx} &= (\lambda + 2\mu)\frac{\partial u_x}{\partial x} + \lambda\frac{\partial u_z}{\partial z}, \\
\sigma_{xz} &= \mu(\frac{\partial u_x}{\partial z} + \frac{\partial u_z}{\partial x}), \\
\sigma_{zz} &= (\lambda + 2\mu)\frac{\partial u_z}{\partial z} + \lambda\frac{\partial u_x}{\partial x},
\end{aligned}
\tag{1}
$$

where σ_{xx} and σ_{zz} are the normal component of stress tensor, σ_{xz} is the shear component. u_x and u_z are displacements in x and z direction. λ is the $Lam\acute{e}$ parameter and μ is the rigidity. λ and μ can be calculated through P wave velocity v_p, S wave velocity v_s and density ρ.

The formulation uses velocity instead of displacement. The velocity is first derivative of displacement with respect to time.

$$
\begin{aligned}
v_x &= \frac{\partial u_x}{\partial t}, \\
v_z &= \frac{\partial u_z}{\partial t},
\end{aligned}
\tag{2}
$$

By taking equation above into equation (1), the relationship between stress and velocity

can be obtained

$$
\begin{aligned}
\frac{\partial \sigma_{xx}}{\partial t} &= (\lambda + 2\mu)\frac{\partial v_x}{\partial x} + \lambda\frac{\partial v_z}{\partial z}, \\
\frac{\partial \sigma_{zz}}{\partial t} &= (\lambda + 2\mu)\frac{\partial v_z}{\partial z} + \lambda\frac{\partial v_x}{\partial x}, \\
\frac{\partial \sigma_{xz}}{\partial t} &= \mu(\frac{\partial v_z}{\partial x} + \frac{\partial v_x}{\partial z}),
\end{aligned}
\tag{3}
$$

It can be inferred from equation (3) that the derivative of stress in one time step can be obtained by velocity wavefield in the past time slice. As a consequence, the stress in the new time slice can be generated.

Newton's second law shows that the acceleration of an object depends on the force and the mass of the object.

$$
F = ma \tag{4}
$$

where F is the force, m is the mass of the object and a is the acceleration of the object. When an external force is absent and only stress is considered, Newton's Second Law turns into

$$
\begin{aligned}
\rho\frac{\partial^2 u_x}{\partial t^2} &= \frac{\partial \sigma_{xx}}{\partial x} + \frac{\partial \sigma_{xz}}{\partial z}, \\
\rho\frac{\partial^2 u_z}{\partial t^2} &= \frac{\partial \sigma_{xz}}{\partial x} + \frac{\partial \sigma_{zz}}{\partial z},
\end{aligned}
\tag{5}
$$

where ρ is the density. By taking equation (2) above into equation (5), the relationship between stress and velocity can be obtained

$$
\begin{aligned}
\frac{\partial v_x}{\partial t} &= \frac{1}{\rho}(\frac{\partial \sigma_{xx}}{\partial x} + \frac{\partial \sigma_{xz}}{\partial z}), \\
\frac{\partial v_z}{\partial t} &= \frac{1}{\rho}(\frac{\partial \sigma_{zz}}{\partial z} + \frac{\partial \sigma_{xz}}{\partial x}),
\end{aligned}
\tag{6}
$$

It can be inferred from equation (6) that the derivative of the velocity in one time step can be obtained by the stress wavefield in the past time slice. As a result, velocity in new time slice can be generated.

Initially, all the stresses and velocity wavefields are zero. The seismic source acts on the stress field. The initial condition and the derivative with respect to time of stress and velocity wavefields are known. So the stress and velocity at any time can be calculated.

METHOD

In an elastic reverse time migration, though the shot wavefield can be separated to generate pure P/S wavefield, a pure P/S seismic source is preferred because the main energy in P/S wavefield increases the quality of imaging.

Examples of pure P/S source

The most commonly used approximation for a pure P wave source is shown in Figure 1. In pure P wave source, only dilatation exists so radial forces come out of the middle point

in all directions. In pure S wave source, only rotation exists, the right two figures show the initial guesses of pure S wave source.
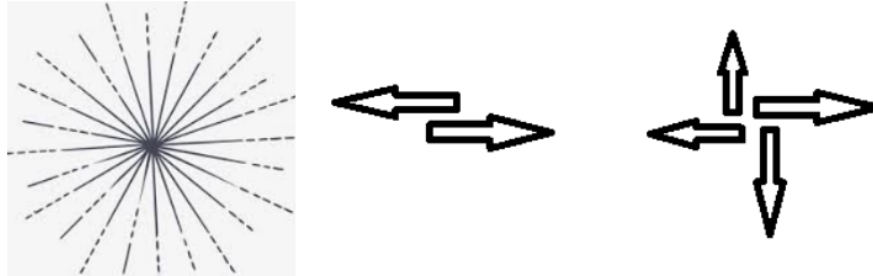

FIG. 1. The initial guess of pure P wave source (left) and pure S wave sources (right two)

For a pure P wave source, each force in one direction can be expressed by a delta function. For example a force with a direction of θ and a length of L in polar coordinates, assuming that the source wavelet is a Ricker wavelet, can be expressed as:

$$f = L * sin(\theta) * wlt * \delta(x - x_i) - L * cos(\theta) * wlt * \delta(z - z_j), \tag{7}$$

where f is the force, (x_i, z_i) is the location of the point source, θ is the polar angle and wlt is the Ricker wavelet. The seismic source is a combination of many single forces.

Typically the pure P wave source is simulated as follows:

$$\begin{bmatrix} fx \\ fz \end{bmatrix} = \begin{bmatrix} \sigma_{xx} & \sigma_{xz} \\ \sigma_{zx} & \sigma_{zz} \end{bmatrix} \begin{bmatrix} n_x \\ n_z \end{bmatrix}, \tag{8}$$

where f_x, f_z are the stress components (surface forces), σ_{xx}, σ_{xz}, σ_{zz} are the components of the stress tensor that reflects the mechanical property of the medium at the source location, n_x, n_z are the unit direction of the force. In this case, they can be expressed as $sin(\theta)$ and $cos(\theta)$.

A pure P wave source stress tensor is commonly set as

$$\begin{aligned} \sigma_{xx} = \sigma_{zz} = wlt, \\ \sigma_{xz} = 0, \end{aligned} \tag{9}$$

If the stress tensor satisfies the equations above, the value of stresses is the same in all directions. But in physics, the seismic source is an external body force instead of a stress, which could be a source of inaccuracy.

An improvement on this approach is as follows: a seismic source acts on a velocity medium as an external force, so if there is a seismic source, equation (5) shall change to

$$\begin{aligned} \rho\frac{\partial^2 u_x}{\partial t^2} = \frac{\partial \sigma_{xx}}{\partial x} + \frac{\partial \sigma_{xz}}{\partial z} + f_x, \\ \rho\frac{\partial^2 u_z}{\partial t^2} = \frac{\partial \sigma_{xz}}{\partial x} + \frac{\partial \sigma_{zz}}{\partial z} + f_z, \end{aligned} \tag{10}$$

where f_z and f_z are external forces of source in x and z direction. In the same way, equation (6) turns into

$$\frac{\partial v_x}{\partial t} = \frac{1}{\rho}(\frac{\partial \sigma_{xx}}{\partial x} + \frac{\partial \sigma_{xz}}{\partial z}) + \frac{f_x}{\rho},$$
$$\frac{\partial v_z}{\partial t} = \frac{1}{\rho}(\frac{\partial \sigma_{zz}}{\partial z} + \frac{\partial \sigma_{xz}}{\partial x}) + \frac{f_z}{\rho}, \tag{11}$$

Dilatation and rotation separation

The P/S wave components can be calculated by Helmholtz decomposition (Aki and Richards, 2002),

$$u_p = \nabla \bullet \mathbf{u} = \frac{\partial u_x}{\partial x} + \frac{\partial u_z}{\partial z},$$
$$\mathbf{u_s} = \nabla \times \mathbf{u} = (\frac{\partial u_x}{\partial z} - \frac{\partial u_z}{\partial x})\mathbf{e}_y, \tag{12}$$

where u_p is dilatation and u_s is rotation, $\mathbf{e}_y$ is the direction of the curl decided by right-hand rule, which is perpendicular to the x-z surface.

For a pure P wave source the $\mathbf{u_s}$ component is zero and for a pure S wave source, the u_p component is zero. A source is a pure P wave source if:

$$\frac{\partial u_x}{\partial z} = \frac{\partial u_z}{\partial x}, \tag{13}$$

which means that for a pure P wave source, the change of u_x in z-direction must be the same as the change of u_z in the x-direction.

An initial approximation of a pure P&S wave is shown in Figure 2. According to equation (12), the divergence at any point of the S wave source and the curl at any point of P wave source should be zero.
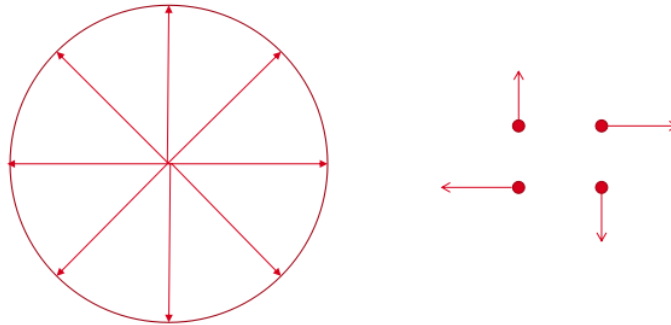

FIG. 2. One initial guess of pure P&S wave source

In the following tests, the first order derivatives are approximated by two points finite difference method. In order to test whether the P/S wave contains S/P wave component or

not, the divergence and curl in the wavefields are computed at the start of the propagation, during which only source points have displacement and all the others are zero.
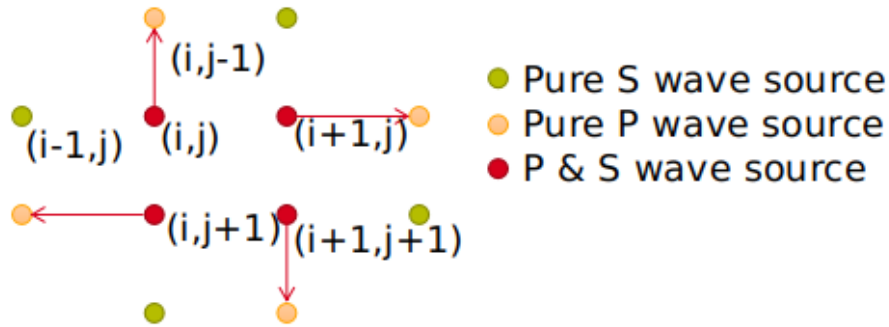

FIG. 3. Points that contains pure P/S wave components and mixed components are displayed in the initial approximation of S wave source

Figure 3 shows the divergence and curl utilizing second order finite difference:

$$u_p(i,j) = \nabla \bullet \mathbf{u} = \frac{\partial u_x(i,j)}{\partial x} + \frac{\partial u_z(i,j)}{\partial z},$$

$$\approx \frac{u_x(i+1,j) - u_x(i-1,j)}{2*\triangle x} + \frac{u_z(i,j+1) - u_z(i,j-1)}{2*\triangle z} = \frac{1}{2*\triangle x} \neq 0,$$

$$|\mathbf{u_s(i,j)}| = |\nabla \times \mathbf{u(i,j)}| = |(\frac{\partial u_x(i,j)}{\partial z} - \frac{\partial u_z(i,j)}{\partial x})\mathbf{e_y}|,$$

$$\approx \frac{u_x(i,j+1) - u_x(i,j-1)}{2*\triangle z} - \frac{u_z(i+1,j) - u_z(i-1,j)}{2*\triangle x} = \frac{-1}{2*\triangle z} \neq 0,$$

(14)

the equations above shows that the divergence and curl of point (i,j) are not zero, which means that point (i,j) is a source point that contains P and S wave components. In the same way, points (i+1,j), (i,j+1), (i+1,j+1) all contain P and S wave components. Points that are pure P wave and pure S wave source are displayed in Figure 3. It can be concluded that the initial approximation of S wave source is actually a mixed P&S wave source. Conclusions may change when the order of finite difference changes.
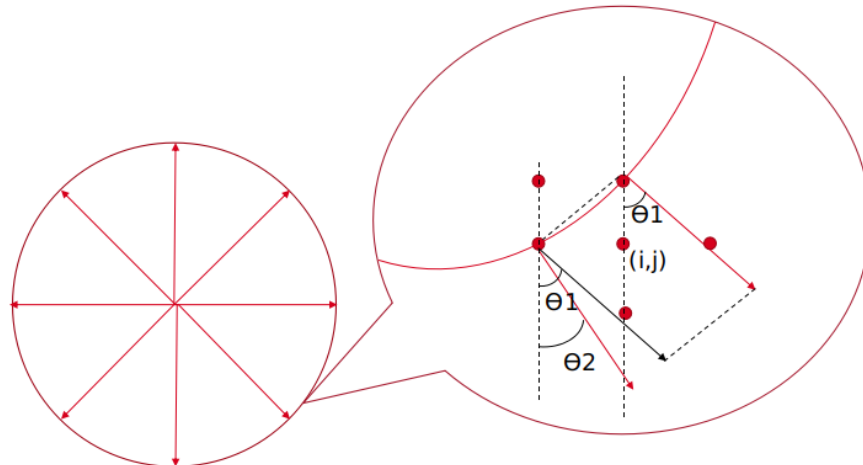

FIG. 4. The initial approximation of pure P wave

In Figure 4 the displacements of two adjacent points on a circle P wave force are displayed. Because the source is in a dial shape, the directions of the two displacements are not the same: $\theta 1 \neq \theta 2$. We calculated the divergence and curl of point(i,j) in Figure 4 :

$$
\begin{aligned}
u_p(i, j) = \nabla \bullet \mathbf{u} &= \frac{\partial u_x(i, j)}{\partial x} + \frac{\partial u_z(i, j)}{\partial z}, \\
&\approx \frac{u_x(i + 1, j) - u_x(i - 1, j)}{2 * \triangle x} + \frac{u_z(i, j + 1) - u_z(i, j - 1)}{2 * \triangle z} \\
&= \frac{-sin(\theta 2)}{2 * \triangle x} + \frac{-sin(\theta 1)}{2 * \triangle z} \neq 0, \\
|\mathbf{u_s(i,j)}| = |\nabla \times \mathbf{u(i,j)}| &= |(\frac{\partial u_x(i, j)}{\partial z} - \frac{\partial u_z(i, j)}{\partial x})\mathbf{e_y}|, \\
&\approx \frac{u_x(i, j + 1) - u_x(i, j - 1)}{2 * \triangle z} - \frac{u_z(i + 1, j) - u_z(i - 1, j)}{2 * \triangle x} \\
&\approx \frac{-cos(\theta 2)}{2 * \triangle z} + \frac{cos(\theta 1)}{2 * \triangle x},
\end{aligned}
\tag{15}
$$

It is apparent that $\theta 1$ and $\theta 2$ have the same positive or negative sign. According to equation (15), the divergence of point (i,j) does not equal to zero. The curl of point (i,j) does not equal to zero on condition that $\frac{\triangle x}{\triangle z} \neq \frac{cos(\theta 1)}{cos(\theta 2)}$. Because $\theta 1$ and $\theta 2$ change in every direction, generally speaking, the S wave components exist in the initial P wave approximation and actually it is a mixed P&S wave source.

But in the stress-velocity method, the displacement can't be obtained directly. As a result, velocity wavefield is utilized since velocity is the derivative of displacement with respect to time. If the change of v_x in the z-direction is the same as the change of v_z in the x-direction, change of u_x in z-direction would be the same as the change of u_z in the x-direction.

RESULTS AND DISCUSSION

P and S wave snapshot

In Figure 5 we show a simulation in homogeneous elastic isotropic medium where v_p is 2km/s and v_s is 1.414km/s and constant density. The seismic source from equation (8) is used. Figure 5 shows the velocity in x and z-direction utilizing the velocity-stress method. We can see that P and S waves are created, but the seismic source used in equation (8) is supposed to be a pure P wave source. It proves that the typical way of creating a pure P wave source is not perfect. The change of v_x in the z-direction is not the same as the change of v_z in the x-direction, as shown in the Figure 6. The Helmholtz decomposition can separate the P and S wave component in velocity wavefield, as shown in Figure 7. A pure P/S wave source can only be created by using a plate source instead of a point source as shown in Figure 8 and 9. In Figure 8 we see the case for a pure P wave source . It can be seen that u_x is always zero in the wavefield, so the change of u_x in the z-direction is zero. And u_z is constant horizontally, so the change of u_z in the x-direction is zero, which fulfills equation (12). The only problem with this source is that on the two ends of the plate pure S wave exists. If the plate is long enough, the S wave created by the plate source can be
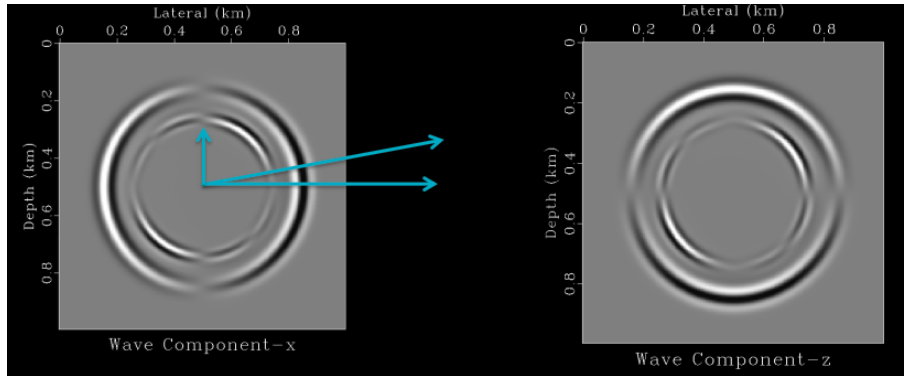
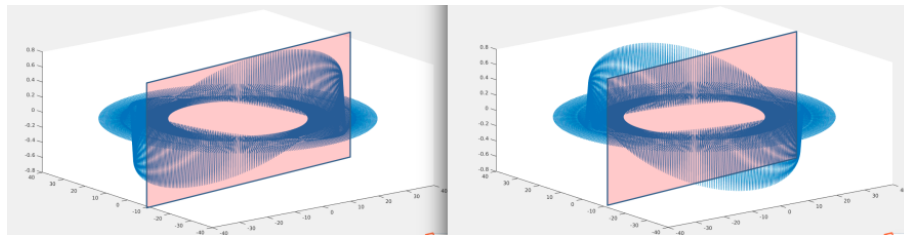FIG. 5. Snapshots of x and z component of velocity in 2D elastic medium

FIG. 6. Snapshots of x(left) and z(right) component of velocity in 2D elastic medium
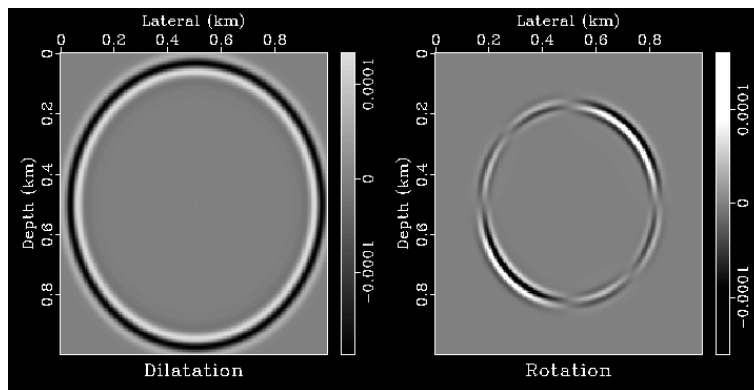

FIG. 7. Snapshots of P wave(left) and S wave(right) component of velocity in 2D elastic medium at 0.27 second. It can be seen that the dilatation and rotation are separated perfectly.
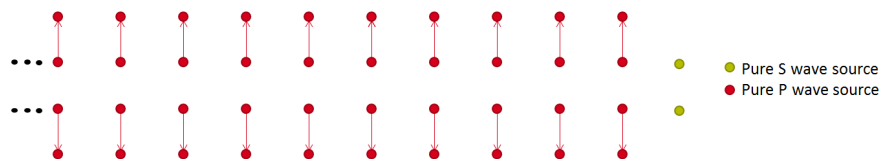

FIG. 8. One part of the pure P wave plate source. The pure P wave sources are denoted by red dots, S wave sources by green dots
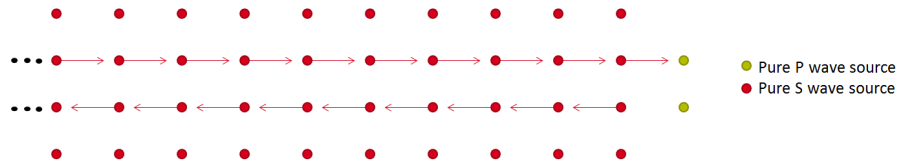
FIG. 9. One part of the pure S wave plate source. The pure S wave sources are denoted by red dots, P wave sources by green dots
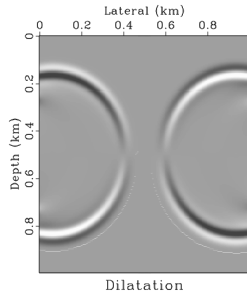

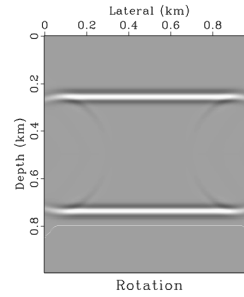FIG. 10. Dilatation of S plate source

FIG. 11. Rotation of S plate source

ignored. Similarly, the pure S wave source can be created using a plate source. In Figure 9, u_z is always zero in the wavefield, so the change of u_z in z direction is zero. u_x is constant horizontally, so the change of u_x in x direction is zero, which fulfills equation (12). The only problem of this source is that on the two ends of the plate pure P wave exists, as shown in Figures 10 and 11. If the plate is long enough, the P wave created by the plate source can be ignored.

In each snapshot the P and S wave component can be obtained, so shot records of P and S wave can be computed by elastic modeling.

P and S wave shot record

To test the P and S energy content for different sources, we generate several records using a 4th order Finite-Difference method and then migrate them using Reverse Time Migration. For these tests, we use acoustic RTM and LSRTM. We created vp and vs model in Figure 12 in order to distinguish the effects of P and S wave, The density model is constant and shares the same size with P wave velocity model. 19 seismic sources from equation (8) are positioned on the surface. One shot record of P and S wave component
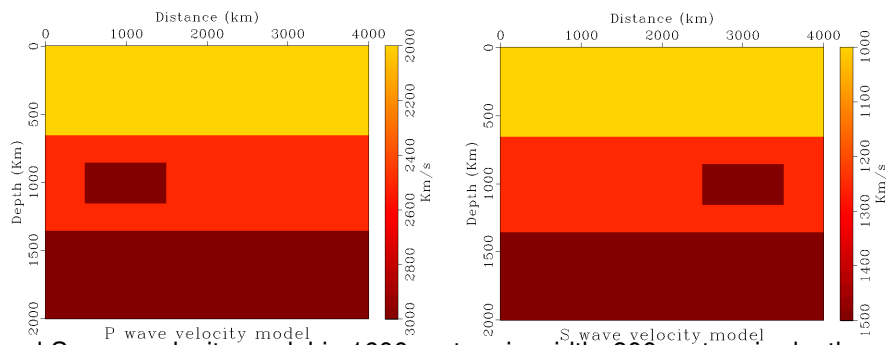

FIG. 12. P and S wave velocity model is 1600 meters in width, 800 meters in depth, grid size is 4 meters vertically and horizontally
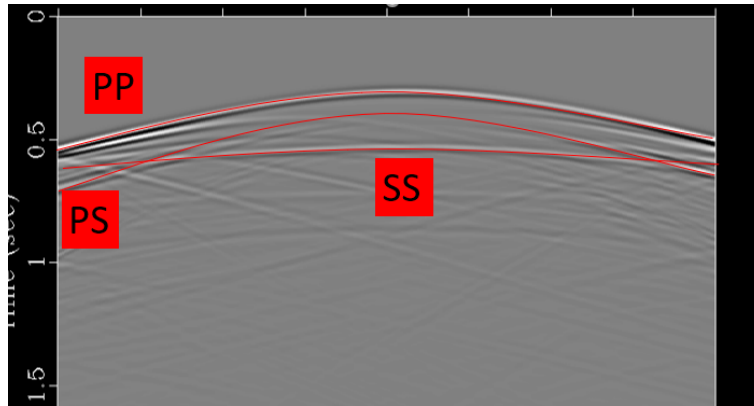
FIG. 13. Shot record of dilatation from mixed P&S wave source. The PP, PS/SP, SS waves calculated from velocity model can be found.
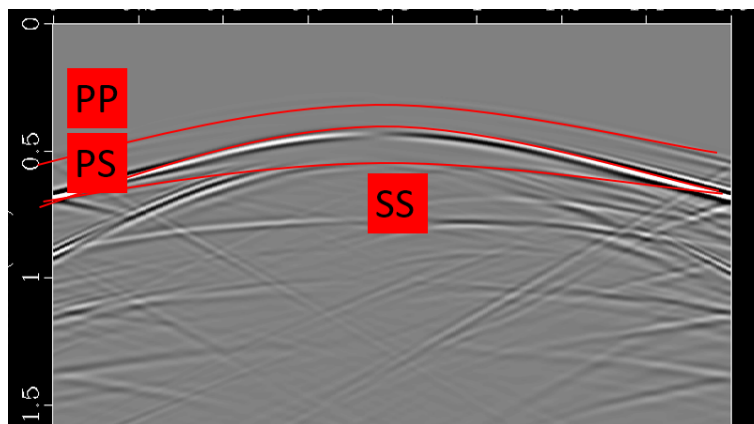

FIG. 14. Shot record of rotation from mixed P&S wave source. The PP, PS/SP, SS waves calculated from velocity model can be found.

are displayed with the direct wave filtered. The PP, PS/SP, and SS waves can be seen in Figures 13 and 14. Theoretically, the PS and SP wave from the first reflector share one event. The absorbing boundary conditions are not perfect because reflection waves can be seen on the left and right boundary.

On the P wave shot record, PP is the strongest reflection wave. The SS wave stands out and is recognized easily. Calculated from the velocity, the PS wave can be recognized but it is very dim.

In Figure 14 we see the S wave record produced by PS and SS reflection waves. PP is noticeable if its position is given. The shot record in Figure 13 should be a combination of PP and SP waves, but the SS wave can be distinguished. The shot record in Figure 14 should be a combination of PS and SS waves, but the PP wave can be distinguished. The PP wave in Figure 14 is so small that can be ignored. This indicates that the Helmholtz decomposition can not separate P and S wave perfectly and the energy in the rotation shot record is small enough to be ignored. Because the PP and SS waves exist, the source contains P and S wave component, which proves the conclusion above that sources formatted from equation (8) are mixed P and S wave source.

Reverse Time Migration

The P and S wave shot records are created by the velocity-stress method (Levander, 1988). Acoustic RTM and Least squares RTM are applied on two shot records separately.
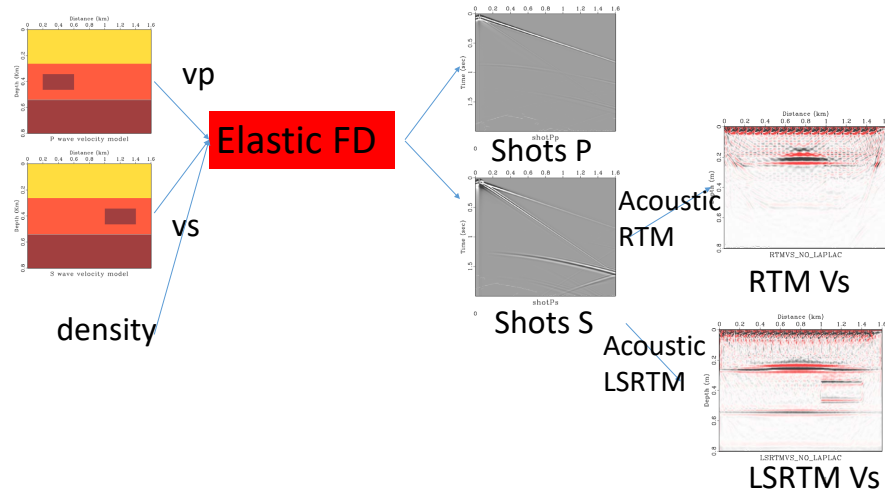

FIG. 15. Work flow

In practice, it is common to use the acoustic RTM and LSRTM instead of the elastic ones because of the high computational cost, as shown in table 1. In 2D acoustic medium, only one wave equation is utilized, but in 2D elastic mediums, five equations are needed: equations (5) & (6). In 3D, this difference is larger because nine equations are needed. A LSRTM running 9 iterations will cost approximately 20 times more than a RTM (2*number of iteration+1). So we use the acoustic RTM and LSRTM.

cost	2D	3D
Acoustic RTM	1	
Acoustic LSRTM	20	
Elastic RTM	5	9
Elastic LSRTM	100	180

Table 1: Comparison of cost on acoustic RTM, acoustic LSRTM, elastic RTM and elastic LSRTM.

Figures 16 and 17 show the results of S wave RTM and least squares RTM.
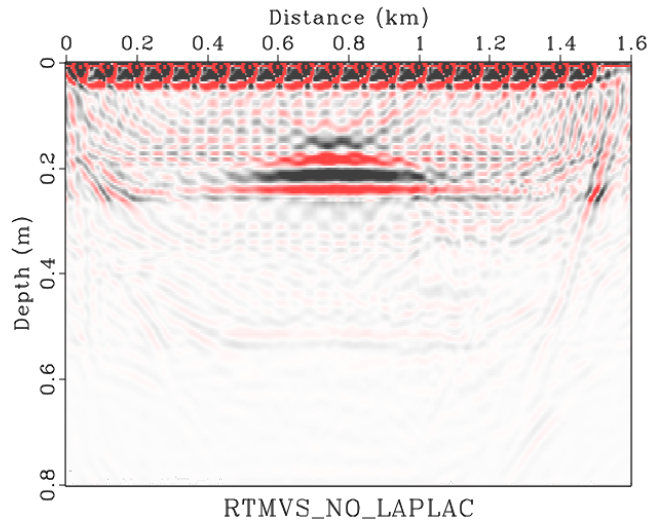
FIG. 16. RTM output from elastic shot records. It contains PS and SS images. PP waves exists on the shot record and set as noise.
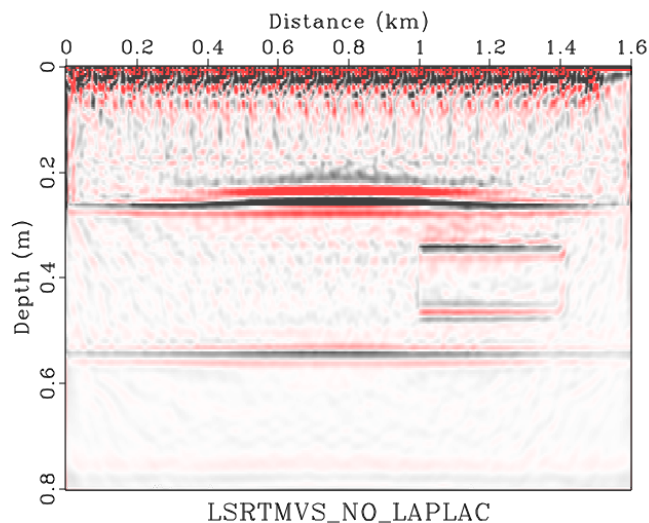

FIG. 17. LSRTM output from elastic shot records. It contains PS and SS images.

By comparing Figures 16 and 17, it can be seen that least squares improve the image significantly. The perturbation in the second layer could barely be seen on the RTM image but on LSRTM it is displayed perfectly. Also, we see the perturbation in the vp model doesn't exist on the LSRTM output. The strong reflector exists on the top of the Figures 16 and 17, which destroys the accuracy. The reason for that is the increase of impedance between the first and second layer is so large that most energy does not transmit to the second layer. In the first and second layer boundary, several events exist in the upwards direction of the accurate position, making the boundary a little "shift up". Because the p wave velocity is larger than the s wave velocity, the PP, PS, SP events are positioned higher than the SS event on the shot record. But the acoustic RTM migrates all the shot record utilizing s wave velocity, so the PP, PS, SP events shifted up the boundary after migration.

Acoustic RTM can only use one velocity model, so for the P wave shot record, the vp is the input velocity model. Similarly, for the S wave shot record, the vs is the input velocity model. But both data sets contain information of vp, vs, and density, so in the RTM of vs model, the P wave component is not migrated to the right position, which can be considered an error. According to Figure 17, the S wave shot record is migrated to the correct vs velocity model, which means that only SS wave is migrated. Compared with RTM results that contain PP, PS, SP and SS events, it can be concluded that least squares could filter the wrong events if the correct velocity model is provided.

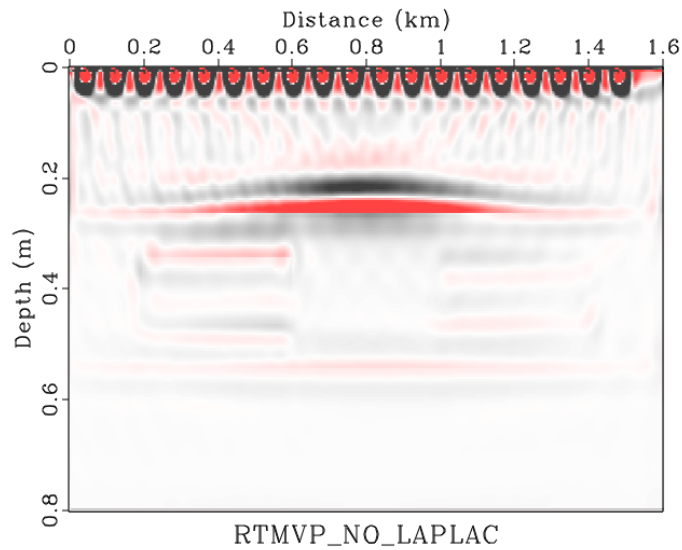Results of P wave RTM and least squares RTM are displayed:

FIG. 18. RTM output from dilatation shot records. It contains PP and SP images. SS waves exists on the shot record and can not ignored.
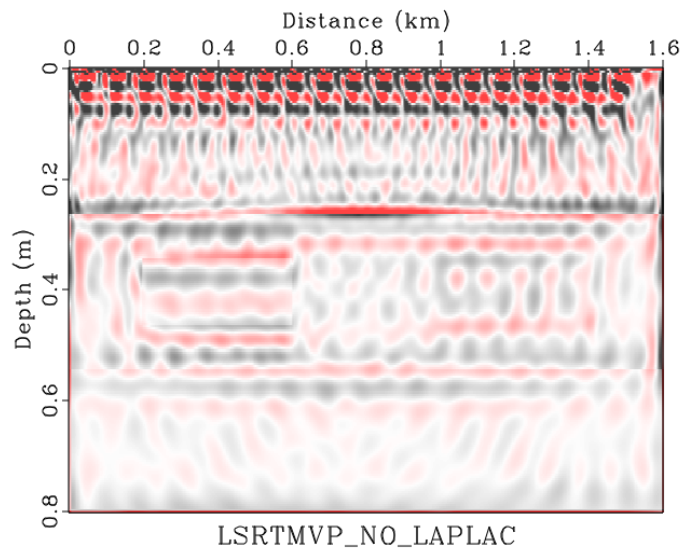

FIG. 19. LSRTM output from dilatation shot records. It contains PP and SP images. SS wave exists on the shot record and could be ignored.

According to Figure 18, it can be seen that perturbation in S wave velocity model exists on P wave RTM results. This may result from the strong SS reflection wave in the P wave shot record. The amplitude in the location of P wave perturbation is larger than that in the S wave perturbation. Two perturbations share reverse polarity. Figure 19 shows the result of P wave LSRTM, which is not satisfying compared with S wave LSRTM. This indicates that when an unwanted wave is strong in the shot record, the filter of least squares may not be that effective. In the P wave LSRTM result, the first reflector and P wave perturbation is surprisingly sharp.

CONCLUSIONS

In an elastic media, the velocity-stress method is commonly utilized to compute various wavefields, which requires a source that preferentially should be a pure P/S source. The usual and simplest method to create a pure P/S wave source is not precise. One possible reason is that the seismic source is created by an external body force instead of stress, which is a surface force. Another reason is that a point source is not accurate to create a pure P/S source compared with a plate source according to the definition of Helmholtz decomposition. The plate source satisfies the condition that there's no dilatation for pure S wave source and no rotation for pure P wave source. But it fails at the two ends of the plate. Helmholtz decomposition is applied in the shot record to separate P and S wave component from velocities gathered from the geophone. It can't separate dilatation and rotation perfectly but the residual can be ignored in the rotation wavefield. To investigate the energy content of the synthetic data, in each case, we use acoustic RTM and LSRTM to calculate the reflectivity images of the elastic medium. As an interesting consequence of these tests, we can see that for the elastic shot records that contain information of vp, vs, and density, S wave acoustic LSRTM could filter the unwanted velocity if the correct velocity model is given.

ACKNOWLEDGMENTS

REFERENCES

Aki, K., and Richards, P., 2002, Quantitative seismology, 2nd ed[]: University Science Books.

Levander, A. R., 1988, Fourth-order finite-difference p-sv seismograms: Geophysics, **53**, 1425–1436.

Virieux, J., 1986, P-SV wave propagation in heterogeneous media: velocity-stress finite-difference method: Geophysics, **51**, 889–901.